

Swift heavy ion irradiation of ZnO nanoparticles embedded in silica: Radiation-induced deoxidation and shape elongation

H. Amekura, N. Okubo, N. Ishikawa, D. Tsuya, K. Mitsuishi et al.

Citation: *Appl. Phys. Lett.* **103**, 203106 (2013); doi: 10.1063/1.4829475

View online: <http://dx.doi.org/10.1063/1.4829475>

View Table of Contents: <http://apl.aip.org/resource/1/APPLAB/v103/i20>

Published by the *AIP Publishing LLC*.

Additional information on *Appl. Phys. Lett.*

Journal Homepage: <http://apl.aip.org/>

Journal Information: http://apl.aip.org/about/about_the_journal

Top downloads: http://apl.aip.org/features/most_downloaded

Information for Authors: <http://apl.aip.org/authors>



Goodfellow

metals • ceramics • polymers
composites • compounds • glasses

Save 5% • Buy online
70,000 products • Fast shipping

Swift heavy ion irradiation of ZnO nanoparticles embedded in silica: Radiation-induced deoxidation and shape elongation

H. Amekura,^{1,a)} N. Okubo,² N. Ishikawa,² D. Tsuya,¹ K. Mitsuishi,¹ Y. Nakayama,¹ U. B. Singh,³ S. A. Khan,³ S. Mohapatra,⁴ and D. K. Avasthi³

¹National Institute for Materials Science (NIMS), Tsukuba, Ibaraki 305-0003, Japan

²Japan Atomic Energy Agency (JAEA), Tokai, Ibaraki, Japan

³Inter-University Accelerator Centre (IUAC), New Delhi, India

⁴Guru Gobind Singh Indraprastha University, New Delhi, India

(Received 6 August 2013; accepted 24 October 2013; published online 11 November 2013)

ZnO nanoparticles (NPs) embedded in amorphous SiO₂ were irradiated with 200 MeV Xe¹⁴⁺ swift heavy ions (SHIs) to a fluence of 5.0×10^{13} ions/cm². Optical linear dichroism was induced in the samples by the irradiation, indicating shape transformation of the NPs from spheres to anisotropic ones. Transmission electron microscopy observations revealed that some NPs were elongated to prolate shapes; the elongated NPs consisted not of ZnO but of Zn metal. The SHI irradiation induced deoxidation of small ZnO NPs and successive shape elongation of the deoxidized metal NPs. © 2013 AIP Publishing LLC. [<http://dx.doi.org/10.1063/1.4829475>]

Nanoparticles (NPs) receive a lot of research attention because of their various fascinating optical,^{1,2} electric,³ and magnetic properties,⁴⁻⁶ which are not observed in their bulk counterparts. These properties can be tuned by controlling the mean size, size distribution, and shapes of the NPs. For shape control of metal NPs, a new approach was discovered in 2003 by D'Orleans *et al.*, who irradiated spherical cobalt NPs embedded in SiO₂ with 200 MeV ¹²⁷I swift heavy ions (SHIs).⁷ They observed deformation of the spherical NPs to lemon-shaped ones at a fluence of about 1×10^{13} ions/cm² and finally to nanorods at about 1×10^{14} ions/cm². One of the fascinating features of this phenomenon is that the NPs are elongated in a direction parallel to the SHI beam; i.e., the elongation direction can be controlled by the SHI beam. Furthermore, all of the NPs are elongated in the same direction. This is important because even if each single elongated NP has anisotropic properties and if its elongation direction cannot be aligned, then the anisotropy of each NP is cancelled out by the summation of a large number of randomly oriented polarizations. Thus, the aligned nature of the elongated NPs fabricated by SHI irradiation could open a new door to the development of anisotropic nanocomposites.

This phenomenon (i.e., shape elongation of embedded NPs) has been confirmed in various *metal* NPs, including Au,⁸⁻¹⁰ Ag,¹¹ Co,⁷ Pt,¹² Zn,¹³ and V,¹⁴ as well as in an ordered alloy of FePt (Ref. 15), and a solid solution of Au_{1-x}Ag_x.¹⁶ Observations of the elongation of non-metallic NPs have, however, been limited to Ge NPs alone.¹⁷ In this paper, we describe the effects of SHI irradiation on another species of non-metallic NPs, i.e., ZnO NPs. Shape elongation of NPs was detected by optical linear dichroism (OLD) spectroscopy and cross-sectional transmission microscopy (XTEM). However, the elongated NPs coexisted with dome-shaped ZnO NPs. Electron energy loss spectroscopy with scanning TEM

(STEM-EELS) revealed that the elongated NPs consisted of Zn metal rather than ZnO.

ZnO NPs were prepared by Zn ion implantation, followed by thermal oxidation.^{18,19} A silica glass of KU-1 type (OH ~ 1000 ppm) was implanted with Zn ions of 60 keV to a fluence of 1.0×10^{17} ions/cm². The implanted samples were annealed at 700 °C for 1 h in flowing oxygen gas. This annealing process induces the formation of the two-layer structure of NPs, i.e., larger ZnO NPs on the surface that are not embedded in SiO₂ and smaller ZnO NPs embedded down to a depth of 10 to 70 nm in SiO₂ (Fig. 1(a)).²⁰ The surface ZnO NPs were covered with a SiO₂ cap-layer of 300 nm by chemical vapor deposition (CVD) at 350 °C.²¹

Samples with embedded ZnO NPs were irradiated with 200 MeV Xe¹⁴⁺ ions by using the Tandem accelerator at the Japan Atomic Energy Agency's Tokai Research and Development Center (JAEA, Tokai). The SHI fluence ranged from 1.0×10^{11} to 5.0×10^{13} ions/cm². The samples were irradiated with an incident angle of 45° from the surface normal because this configuration has been found to be appropriate for the detection of particle elongation by OLD spectroscopy.¹³ A dual-beam spectrophotometer was used for OLD spectroscopy in the wavelength region of 215–800 nm at room temperature (RT) with an optical polarizer (extinction ratio $< 5 \times 10^{-5}$). The optical transmission at certain polarization angles was measured, and the results were plotted in the form of optical density (OD) without correction for reflection, i.e., $OD = -\log_{10} T$, where T denotes the transmittance. XTEM was carried out at an acceleration voltage of 200 kV. Bright field, high-angle annular dark field (HAADF), and STEM-EELS observations were carried out.

Figure 2 shows the OD spectra of ZnO NPs with a SiO₂ cap-layer, as detected by using linearly polarized light. The spectra were recorded at polarization angles of 0° (P-polarization) and 90° (S-polarization), where the polarization plane of 0° is defined as the plane containing the SHI beam trajectories.¹³ Oscillating structures are ascribed mainly to interference fringes due to the cap-layer. Before SHI irradiation, a steep edge was observed at about 3.3 eV in

^{a)}Author to whom correspondence should be addressed. Electronic mail: amekura.hiroshi@nims.go.jp. Tel.: +81-29-863-5477. Fax: +81-29-863-5599.

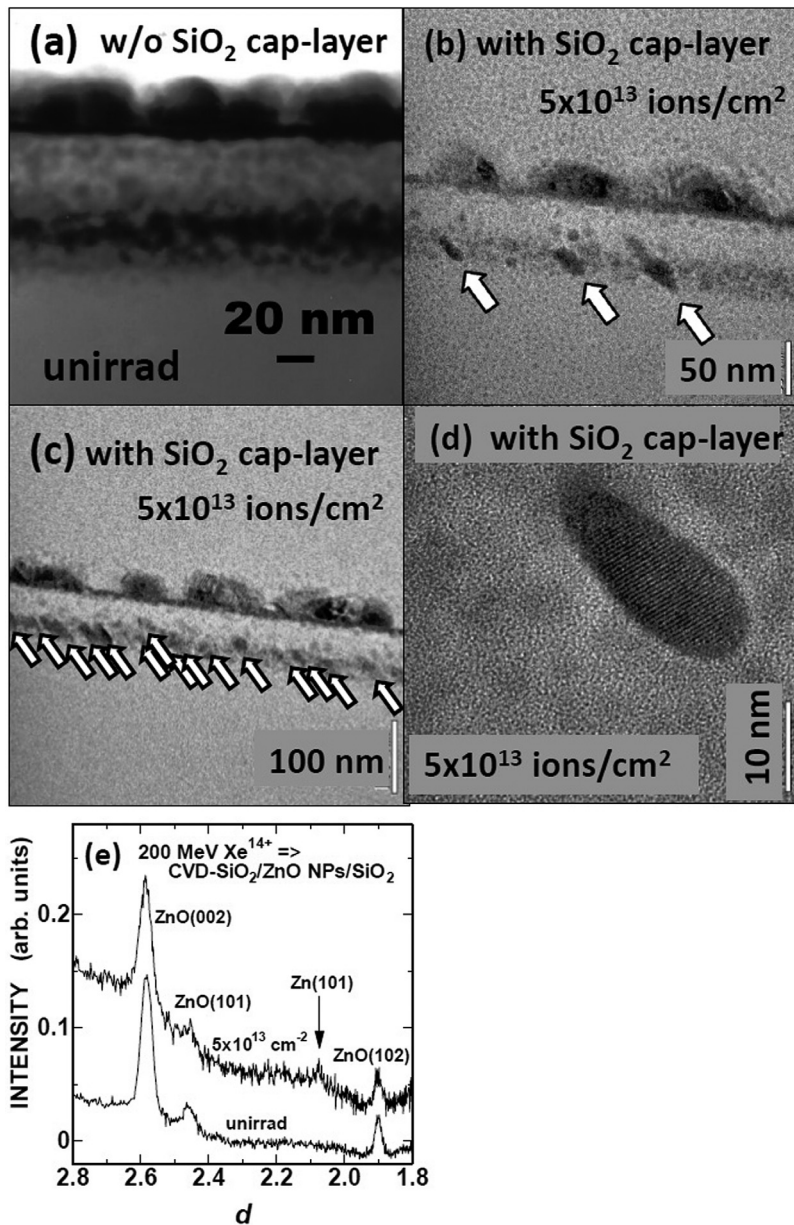


FIG. 1. Bright-field cross-sectional TEM images of ZnO NPs without a SiO₂ cap-layer in an unirradiated state (a) and of those with a cap-layer after irradiation with 200 MeV Xe¹⁴⁺ ions to a fluence of 5.0×10^{13} ions/cm² (b) and (c). Image (b) shows dome-like ZnO NPs with small satellites and elongated NPs, and (d) is a high-resolution image of an elongated NP. Elongated NPs in (b) and (c) are shown by arrows. Diffraction patterns are shown in (e) for the unirradiated state and after irradiation to 5.0×10^{13} ions/cm².

the OD spectrum; this was ascribed to the free-exciton absorption edge of ZnO NPs. In fact, this edge was also observed in a sample without the cap-layer. Because the sizes of the surface ZnO NPs and of the embedded NPs were 30–50 nm and ~ 10 nm, respectively, both of them were much larger than the exciton Bohr radius (~ 2 nm) of bulk ZnO (Ref. 22); consequently, a pronounced quantum size effect of the excitons was not expected.

With increasing fluence, the exciton edge became broader and shifted to the high energy side. The OLD signal, i.e., polarization-dependent absorption, was observed at about 2.5–4.3 eV and 1.5–4.1 eV for samples irradiated at 1.0×10^{13} and 5.0×10^{13} ions/cm², respectively. The observed OLD could be ascribed to elongation of the NPs. However, it is not clear why the OLD was observed not only above the band-gap (3.3 eV) of ZnO NPs but also below the band-gap. The OLD below the band-gap of ZnO NPs cannot be explained in terms of ZnO but is easy to understand if elongated Zn metal particles are present. A diffraction peak from the Zn metal phase appeared after the SHI irradiation (Fig. 1(e)).

To confirm the elongation of NPs, XTEM observation was conducted. A bright field image from the sample irradiated to a fluence of 5.0×10^{13} ions/cm² is shown in Figs. 1(b) and 1(c). The bigger NPs with dome-like shapes located at the upper center of Fig. 1(b) were originally the surface ZnO NPs. Similar images were observed in Fig. 1(a) before SHI irradiation. In fact, the original SiO₂ surface before the cap-layer deposition is clearly visible as a black horizontal line around the center of Fig. 1(b). Around the dome-shaped ZnO NPs, some small satellite NPs are visible; these could have contributed to the broadening and high-energy shift of the exciton edge of the NPs via the quantum size effect. Formation of satellite NPs is a relatively common feature of embedded NPs irradiated with ~ 100 keV ions,^{23,24} \sim MeV ions,²⁵ or SHIs.^{16,26} The satellite NPs are evidence of mass transport between the NPs and the matrix, i.e., they indicate that the ZnO NPs were partly dissolved into the matrix owing to the SHI irradiation. Elongated NPs were observed approximately 50 nm deeper than the original substrate surface, where smaller embedded ZnO NPs once existed before

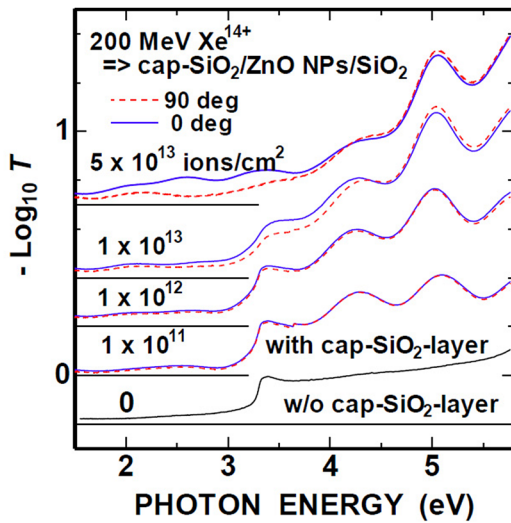


FIG. 2. Optical density spectra of ZnO nanoparticles on a silica substrate with a SiO₂ cap-layer, after irradiation with 200 MeV Xe¹⁴⁺ ions to four different fluences. Linearly polarized light with P-polarization (0°) and S-polarization (90°) was applied. Details of the geometry are given in Ref. 35. For comparison, the spectrum of an unirradiated sample without the cap-layer is shown. The spectra at the different fluences were vertically shifted from each other; horizontal lines indicate baselines.

the irradiation. The major axes of the elongated NPs were pointing in the same direction, i.e., in the incident direction of the SHI beam at 45° from the surface normal. Figure 1(c) shows that the elongated NPs are not accidental and rare products but are observable in many places.

A high-resolution TEM image (HR-TEM) of an elongated NP is shown in Fig. 1(d). Lattice fringes with a period of 0.495 nm were observed and could be ascribed to Zn (001) diffraction. Although the fringe could be assigned to the second harmonics of 0.2476-nm diffraction of ZnO (101), this possibility is excluded by the following STEM-EELS results.

To judge more clearly whether the elongated NPs were made of ZnO or Zn, we performed a composition analysis using STEM-EELS. Figure 3(a) is an HAADF image of the area around an elongated NP indicated by “1”; it clearly shows the elongated NP, as well as nearly spherical NPs around it. Figure 3(b) shows the element compositions (Zn, Si, and O) detected by STEM-EELS along the line shown in Fig. 3(a). The Zn peaks appearing at positions $x \sim 14$ and 48 nm correspond to a nearly spherical NP and the elongated one, respectively. From the concentration profiles of Zn, Si, and O shown in Fig. 3(b), the profile of a metallic Zn element was determined (Fig. 3(c)), under the assumption of stoichiometric ZnO and SiO₂. The result showed that the elongated NP at $x \sim 48$ nm and the nearly spherical NP at ~ 14 nm consisted of Zn metal and ZnO, respectively.

The presence of elongated metallic NPs is also consistent with the OLD signal observed in Fig. 2: the observation of an OLD signal at the photon energies both above and below the band-gap of ZnO can be reasonably explained if the OLD signal is from elongated Zn metal NPs. According to a previous observation, elongated Zn NPs show an OLD down to 1.5 eV or less.¹³ Furthermore, the evolution of the OD spectra with increasing fluence can be ascribed to the deoxidation of ZnO NPs and the reduction in size of the ZnO

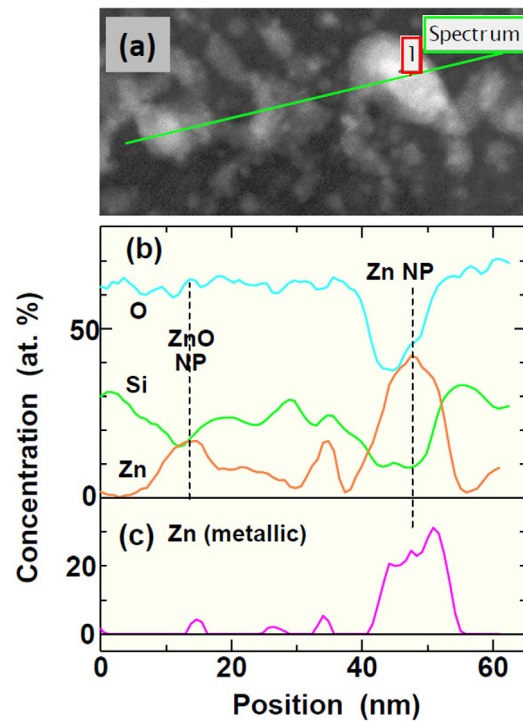
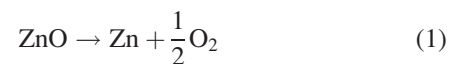


FIG. 3. (a) HAADF image of an elongated NP (indicated by “1”) observed in a ZnO NP sample with a cap-layer; the sample was irradiated with 200 MeV Xe¹⁴⁺ ions to a fluence of 5.0×10^{13} ions/cm². (b) Elemental distributions of Zn, Si, and O atoms along the line shown in (a) across the NP, as detected by STEM-EELS. (c) Distribution of metallic Zn, as determined under the assumption of stoichiometric ZnO and SiO₂.

parts. While the OD spectrum in the region between 3.5 and 4.5 eV was almost constant before irradiation, it increased with increasing photon energy after irradiation at a fluence higher than 1×10^{12} ions/cm²; this result was similar to the case with Zn NPs.¹³

According to thermodynamics data,²⁷ the standard Gibbs energy change $\Delta G^0(T)$ of the thermal deoxidation reaction of



is a positive value of +350 kJ/mol at 300 K, i.e., the reaction is not spontaneously driven at 300 K. However, the $\Delta G^0(T)$ decreases with increasing temperature. When 2350 K is exceeded, $\Delta G^0(T)$ becomes negative, i.e., the deoxidation reaction is spontaneously driven. Although this temperature is transiently accessible with the thermal spike effect of 200 MeV Xe ions in SiO₂, the critical issue is whether or not the duration of heat at $T > 2350$ K is long enough for the reaction.

Larger ZnO NPs on the ex-surface are not transformed, but some of the smaller NPs below the ex-surface are transformed to elongated NPs (Fig. 1(b)). It has already been suggested by D’Orleans *et al.*⁷ that the temperature increases to higher levels in the case of smaller NPs, even under the same conditions of irradiation. A spherical NP with a diameter of $2R$ gains energy of ε

$$\varepsilon = S_e (= dE/dx) \times 2R, \quad (2)$$

when an SHI goes through the center of the NP. Soon the energy is shared by the volume of the NP, i.e., $V = (4\pi/3)R^3$. Consequently, the energy density ε/V

$$\varepsilon/V = (3/2\pi)S_{\varepsilon}/R^2 \quad (3)$$

is proportional to $1/R^2$: the smaller the NP, the larger the energy density. In this context, amorphous SiO₂ plays an important role as an excellent heat-insulating matrix. This is a probable reason why the smaller NPs show deoxidation but the larger ones do not. The heat conductivity of silica (amorphous SiO₂) is 0.014 W cm⁻¹ K⁻¹, i.e., ~100 times smaller than that of ZnO at ~1.0 W cm⁻¹ K⁻¹. There have been no reports of SHI-irradiation-induced deoxidation of bulk ZnO crystals and thin films. In fact, ZnO NPs of typically 50 nm length and 21 nm diameter have been irradiated with 120 MeV Ag⁹⁺ ions to a fluence of 9×10^{10} ions/cm²: only fragmentation, not deoxidation, is induced,²⁸ consistent with the results for the larger ZnO NPs in our samples. A configuration of small particles separated by SiO₂, an excellent heat-insulator, is essential to increase temperature and thus induce the reaction (1).

Phase separation and subsequent formation of mono-element nano-phases of Si, Ge, and In have been reported in the case of non-stoichiometric SiO_x,²⁹ GeO_x,^{30,31} and In_xO_y (Ref. 32) irradiated with SHIs. However, the mechanism could differ from that in our case. Non-stoichiometry plays an important role in these systems. In contrast, it has been confirmed from X-ray photoelectron spectroscopy,³³ optical absorption spectroscopy,³⁴ and X-ray diffraction³⁴ that almost no Zn NPs exist before SHI irradiation, i.e., in our case the reaction is stoichiometric.

In summary, ZnO NPs embedded in SiO₂ were irradiated with 200 MeV Xe¹⁴⁺ ions up to 5.0×10^{13} ions/cm². Anisotropic optical absorption (i.e., OLD) and elongated morphology of NPs were observed. Furthermore, the elongated NPs were not ZnO, but Zn metal. SHI irradiation induces deoxidation of ZnO NPs to Zn NPs as a consequence of a deoxidation reaction (1) driven by the thermal spike effect but enhanced by the small geometry of the NPs embedded in thermally insulating silica. In the course of deoxidation, the ZnO NPs are divided into smaller domains separated by metallic Zn or defects, which contribute to the broadening and blue-shift of the exciton edge via the quantum size effect. Finally, shape elongation is induced in the deoxidized Zn NPs.

This work was supported by the Bilateral Joint Research Project between JSPS-Japan and DST-India (DST/INT/JSPS/P-111/2011). The SHI irradiation was partly performed under the Common-Use Facility Program of JAEA. A part of this study was supported by “Nanotechnology Network Project” of the Ministry of Education, Culture, Sports, Science and Technology (MEXT), Japan. The authors also thank Professor S. Mantl and Mr. A. Dahmen (FZ Juelich) for Zn ion implantation and Mr. M. Ochiai (NIMS) for CVD.

¹R. F. Haglund, L. Yang, R. H. Magruder, C. W. White, R. A. Zuhr, L. Yang, R. Dorsinville, and R. R. Alfano, *Nucl. Instrum. Methods Phys. Res. B* **91**, 493 (1994).

²U. Kreibig and M. Vollmer, *Optical Properties of Metal Clusters* (Springer-Verlag, Berlin, Heidelberg, New York, 1995).

³A. Nakajima, H. Nakao, H. Ueno, T. Futatsugi, and N. Yokoyama, *Appl. Phys. Lett.* **73**, 1071 (1998).

⁴M. Solzi, M. Ghidini, and G. Asti, in *Magnetic Nanostructures*, edited by H. S. Nalwa (American Sci. Pub., Valencia, CA, USA, 2002), p. 123.

⁵H. Amekura, H. Kitazawa, N. Umeda, Y. Takeda, and N. Kishimoto, *Nucl. Instrum. Methods Phys. Res. B* **222**, 114 (2004).

⁶H. Amekura, Y. Fudamoto, Y. Takeda, and N. Kishimoto, *Phys. Rev. B* **71**, 172404 (2005).

⁷C. D’Orleans, J. P. Stoquert, C. Estournès, C. Cerruti, J. J. Grob, J. L. Guille, F. Haas, D. Muller, and M. Richard-Plouet, *Phys. Rev. B* **67**, 220101 (2003).

⁸S. Roorda, T. van Dillen, A. Polman, C. Graf, A. van Blaaderen, and B. J. Kooi, *Adv. Mater.* **16**, 235 (2004).

⁹Y. K. Mishra, F. Singh, D. K. Avasthi, J. C. Pivin, D. Malinowska, and E. Pippel, *Appl. Phys. Lett.* **91**, 063103 (2007).

¹⁰K. Awazu, X. Wang, M. Fujimaki, J. Tominaga, H. Aiba, Y. Ohki, and T. Komatsubara, *Phys. Rev. B* **78**, 054102 (2008).

¹¹A. Oliver, J. A. Reyes-Esqueda, J. C. Cheang-Wong, C. E. Roman-Velazquez, A. Crespo-Sosa, L. Rodríguez-Fernandez, J. A. Seman, and C. Noguez, *Phys. Rev. B* **74**, 245425 (2006).

¹²R. Giuliani, P. Kluth, L. L. Araujo, D. J. Sprouster, A. P. Byrne, D. J. Cookson, and M. C. Ridgway, *Phys. Rev. B* **78**, 125413 (2008).

¹³H. Amekura, N. Ishikawa, N. Okubo, M. C. Ridgway, R. Giuliani, K. Mitsuishi, Y. Nakayama, Ch. Buchal, S. Mantl, and N. Kishimoto, *Phys. Rev. B* **83**, 205401 (2011).

¹⁴H. Amekura, N. Ishikawa, N. Okubo, Y. Nakayama, and K. Mitsuishi, *Nucl. Instrum. Methods Phys. Res. B* **269**, 2730 (2011).

¹⁵M. Shirai, K. Tsumori, M. Kutsuwada, K. Yasuda, and S. Matsumura, *Nucl. Instrum. Methods Phys. Res. B* **267**, 1787 (2009).

¹⁶G. Rizza, F. Attouchi, P. E. Coulon, S. Perruchas, T. Gacoin, I. Monnet, and L. Largeau, *Nanotechnology* **22**, 175305 (2011).

¹⁷B. Schmidt, K. H. Heinig, A. Muecklich, and C. Akhmedaliev, *Nucl. Instrum. Methods Phys. Res. B* **267**, 1345 (2009).

¹⁸H. Amekura, N. Umeda, Y. Sakuma, N. Kishimoto, and Ch. Buchal, *Appl. Phys. Lett.* **87**, 013109 (2005).

¹⁹H. Amekura and N. Kishimoto, in *Lecture Notes in Nanoscale Science and Technology*, edited by Z. Wang (Springer, New York, 2009), Vol. 5, pp. 1–75.

²⁰H. Amekura, N. Umeda, Y. Sakuma, O. A. Plaksin, Y. Takeda, N. Kishimoto, and Ch. Buchal, *Appl. Phys. Lett.* **88**, 153119 (2006).

²¹For comparison, samples without the SiO₂ cap-layers were also irradiated under the same conditions. However, OLD signal, i.e., the elongation of NPs, was not observed.

²²H. Morkoc and U. Ozgur, *Zinc Oxide* (Wiley-VCH Verlag GmbH & Co. KGaA, Weinheim, 2009).

²³G. Mattei, G. D. Marchi, C. Maurizio, P. Mazzoldi, C. Sada, V. Bello, and G. Battaglin, *Phys. Rev. Lett.* **90**, 085502 (2003).

²⁴G. Pellegrini, V. Bello, G. Mattei, and P. Mazzoldi, *Opt. Express* **15**, 10097 (2007).

²⁵G. Rizza, Y. Ramjauny, T. Gacoin, L. Vieille, and S. Henry, *Phys. Rev. B* **76**, 245414 (2007).

²⁶M. C. Ridgway, P. Kluth, R. Giuliani, D. J. Sprouster, L. L. Araujo, C. S. Schnohr, D. J. Llewellyn, A. P. Byrne, G. J. Foran, and D. J. Cookson, *Nucl. Instrum. Methods Phys. Res. B* **267**, 931 (2009).

²⁷O. Kubaschewski, E. L. Evans, and C. B. Alcock, *Metallurgical Thermochemistry*, 4th ed. (Pergamon, London, 1967).

²⁸S. Bayan and D. Mohanta, *Physica E* **54**, 288 (2013).

²⁹W. M. Arnoldbik, N. Tomozeiu, E. D. van Hattum, R. W. Lof, A. M. Vredenberg, and F. H. P. M. Habraken, *Phys. Rev. B* **71**, 125329 (2005).

³⁰Y. Batra, D. Kabiraj, S. Kumar, and D. Kanjilal, *J. Phys. D: Appl. Phys.* **40**, 4568 (2007).

³¹S. Rath, D. Kabiraj, D. K. Avasthi, A. Tripathi, K. P. Jain, M. Kumar, H. S. Mavi, and A. K. Shukla, *Nucl. Instrum. Methods Phys. Res. B* **263**, 419 (2007).

³²N. Tripathi, S. Rath, P. K. Kulriya, S. A. Khan, D. Kabiraj, and D. K. Avasthi, *Nucl. Instrum. Methods Phys. Res. B* **268**, 3335 (2010).

³³H. Amekura, N. Umeda, M. Yoshitake, K. Kono, N. Kishimoto, and Ch. Buchal, *J. Cryst. Growth* **287**, 2 (2006).

³⁴H. Amekura, K. Kono, N. Kishimoto, and Ch. Buchal, *Nucl. Instrum. Methods Phys. Res. B* **242**, 96 (2006).

³⁵H. Amekura, M. L. Sele, N. Ishikawa, and N. Okubo, *Nanotechnology* **23**, 095704 (2012).